European Journal of Pharmaceutical Sciences 168 (2022) 106034

Contents lists available at ScienceDirect

European Journal of Pharmaceutical Sciences

journal homepage: www.elsevier.com/locate/ejps

On the usefulness of four in vitro methods in assessing the intraluminal performance of poorly soluble, ionisable compounds in the fasted state

Patrick J O'Dwyer [a,b,c], Karl J Box [a], Georgios Imanidis [d,e], Maria Vertzoni [b], Christos Reppas [b,*]

[a] Pion Inc. (UK) Ltd., Forest Row, East Sussex, United Kingdom
[b] Department of Pharmacy, School of Health Sciences, National and Kapodistrian University of Athens, Zografou, Greece
[c] School of Pharmacy, University College Cork, College Road, Cork, Ireland
[d] University of Applied Sciences Northwest. Switzerland. School of Life Sciences, Institute of Pharma Technology, Hofackerstrasse 30, 4132 Muttenz, Switzerland
[e] University of Basel, Department of Pharmaceutical Sciences, Basel, Switzerland

ARTICLE INFO

Keywords:
Dissolution
Precipitation
PBPK modelling
Biphasic
Dissolution-permeation
Biogit

ABSTRACT

A small-scale two-stage biphasic system, a small-scale two-stage dissolution-permeation system, the Erweka mini-paddle apparatus, and the BioGIT system were evaluated for their usefulness in assessing the intraluminal performance of two low solubility drugs in the fasted state, one with weakly acidic properties (tested in a salt form, diclofenac potassium) and one with weakly alkaline properties [ritonavir, tested as an amorphous solid dispersion (ASD) formulation].

In all *in vitro* methods, an immediate-release tablet and a powder formulation of diclofenac potassium were both rapidly dissolved in Level II biorelevant media simulating the conditions in the upper small intestine. Physiologically based biopharmaceutics (PBB) modelling for the tablet formulation resulted in a successful simulation of the average plasma profile in adults, whereas for the powder formulation modelling indicated that gastric emptying and transport through the intestinal epithelium limit the absorption rates.

Detailed information on the behaviour of the ritonavir ASD formulation under both simulated gastric and upper small intestinal conditions were crucial for understanding the luminal performance. PBB modelling showed that the dissolution and precipitation parameters, estimated from the Erweka mini-paddle apparatus data and the small-scale two-stage biphasic system data, respectively, were necessary to adequately simulate the average plasma profile after administration of the ritonavir ASD formulation. Simulation of the gastrointestinal transfer process from the stomach to the small intestine was necessary to evaluate the effects of hypochlorhydric conditions on the luminal performance of the ritonavir ASD formulation.

Based on this study, the selection of the appropriate *in vitro* method for evaluating the intraluminal performance of ionisable lipophilic drugs depends on the characteristics of the drug substance. The results suggest that for (salts of) acidic drugs (e.g., diclofenac potassium) it is only an issue of availability and ease of operation of the apparatus. For weakly alkaline substances (e.g., ritonavir), the results indicate that the dynamic dissolution process needs to be simulated, with the type of requested information (e.g., dissolution parameters, precipitation parameters, luminal concentrations) being key for selecting the most appropriate method. Regardless of the ionisation characteristics, early in the drug development process the use of small-scale systems may be inevitable, due to the limited quantities of drug substance available.

1. Introduction

Oral drug absorption is a complex process which can be influenced by many factors. These can be related to the underlying physiology of the gastrointestinal (GI) tract, the properties of the drug molecule and the drug formulation behaviour. These factors directly affect the absorption of drug and, therefore, its bioavailability. The appropriate use of *in vitro* tools is a critical challenge for the pharmaceutical industry when evaluating the oral absorption of new drugs. Obtaining biorelevant information on the performance of formulations can reduce the

* To whom correspondence should be addressed: Department of Pharmacy, School of Health Sciences, National and Kapodistrian University of Athens, Panepistimiopolis, 157 71 Zografou, Greece.
E-mail address: reppas@pharm.uoa.gr (C. Reppas).

https://doi.org/10.1016/j.ejps.2021.106034
Received 16 June 2021; Received in revised form 3 September 2021; Accepted 5 October 2021
Available online 7 October 2021
0928-0987/© 2021 The Authors. Published by Elsevier B.V. This is an open access article under the CC BY-NC-ND license (http://creativecommons.org/licenses/by-nc-nd/4.0/).

cost of drug development, decrease the amount of *in vivo* studies required and cut the time taken to reach the market. Various small- and full-scale *in vitro* methods to assess the luminal performance of solid drug products have been proposed, however, in many cases, their usefulness has not been fully explored (O'Dwyer et al., 2019). In addition, comparative evaluation of proposed *in vitro* methods from literature data is hindered by the use of different drug substances, formulations, and doses tested in the published studies.

In this study, we evaluated the usefulness of a small-scale two-stage biphasic system (Jankovic et al., 2019; O'Dwyer et al., 2020), a small-scale two-stage dissolution-permeation (D-P) system (O'Dwyer et al., 2020), the Erweka (Heusenstamm, Germany) mini-paddle apparatus, and the biorelevant gastrointestinal transfer (BioGIT) system (Kourentas et al., 2018) in assessing the intraluminal performance of poorly soluble, ionisable compounds in the fasted state. This assessment was completed either indirectly after incorporating *in vitro* data into physiologically based biopharmaceutics (PBB) models and simulating the plasma profiles (Jamei et al., 2020), or directly by comparing *in vitro* with luminal data. In this study, the luminal performance of formulations of two ionizable drug substances (diclofenac potassium and ritonavir) were examined. While the Erweka mini-paddle apparatus is considered to be a small-scale setup in previous works (Klein and Shah, 2008), in pharmaceutical profiling and early formulation development an even smaller scale can be beneficial. Therefore, in this article the Erweka mini-paddle apparatus is not categorised as a small-scale method, given the volume of water (250 mL) administered with a dose in clinical studies.

Diclofenac is a Biopharmaceutics Classification System (BCS) Class II weak acid (pKa 3.8) (Guhmann et al., 2013). The impact of formulation on the luminal performance of diclofenac potassium was appraised. Salts of low solubility weak acids may lead to precipitation of the free acid in the stomach due to pH-dependant solubility, with subsequent potential complications in the oral drug absorption process (Guhmann et al., 2013; Van Den Abeele et al., 2017, 2016). However, if the residence time in the stomach is short or rapid redissolution occurs in the intestine, precipitation may not be clinically significant. Two products containing the potassium salt of diclofenac were tested: an immediate-release tablet (Cataflam®) and powder for oral solution formulation (Voltfast®). *In vitro* data were used for the simulation of plasma profiles which were then evaluated versus previously published actual plasma data in adults (Marzo et al., 2000) or they were compared with previously published luminal data in adults (Van Den Abeele et al., 2017).

Ritonavir is a BCS class IV weak base (basic pKas = 1.8, 2.6) (Xu et al., 2017). The luminal performance of a ritonavir amorphous solid dispersion (ASD) tablet (Norvir®) was evaluated under conditions simulating normal and reduced gastric acid secretion in the fasted state. Due to the amorphous ritonavir state, supersaturation can occur in the stomach and, especially, in the increased pH of the lumen of the upper small intestine. The concept has been applied to various lipophilic weak bases (Brouwers et al., 2017; Litou et al., 2020; Xu et al., 2017) to achieve adequate oral bioavailability. However, supersaturated states are thermodynamically unstable and the degree of supersaturation is the driving force for precipitation (Brouwers et al., 2009; Hens et al., 2016; Psachoulias et al., 2011). As with diclofenac potassium, in this study *in vitro* ritonavir data were used for the simulation of plasma profiles which were then evaluated versus previously published actual plasma data in adults (Ng et al., 2008) or they were compared with previously published luminal data in adults (Van Den Abeele et al., 2020).

2. Materials and methods

2.1. Materials

Diclofenac free acid (> 98.0%) and diclofenac potassium (> 98.0%) were received from Kemprotec (Cumbria, UK), to obtain the standard UV spectra for the *in situ* tests and for the standard curves. Cataflam® 50 mg IR film-coated immediate release tablets (Novartis Ireland Limited, Dublin, Ireland), and Voltfast® 50 mg powder for oral solution (Novartis Pharma Schweiz AG, Rotkreuz) were obtained from community pharmacy sources, with lot number and expiry dates provided in the Supplementary materials (Table S1). Both formulations contain 50 mg of diclofenac potassium, equivalent to 44.3 mg of the free acid.

Ritonavir (≥ 98%) was obtained from Sigma-Aldrich (Dorset, UK). Norvir® 100 mg film-coated tablets (AbbVie Deutschland GmbH & Co. KG, Ludwigshafen) was obtained from community pharmacy sources, with lot number and expiry dates provided in the Supplementary materials (Table S1). Norvir® film-coated tablet is an ASD in a polyvinylpyrrolidone – vinyl acetate copolymer matrix (Xu et al., 2017).

Acceptor Sink Buffer (ASB), consisting of a HEPES buffer at pH 7.4 along with surfactants, and GIT (Gastrointestinal Tract) Lipid Solution (20% lecithin in dodecane lipid solution) were received from Pion Inc (MA, USA). SIF powder and Fasted State Simulated Intestinal Fluid (FaSSIF) V2 (Bou-Chacra et al., 2017) powder were obtained from biorelevant.com (London, UK). Decanol was purchased from Alfa Aesar (Heysham, UK). Hard gelatine capsules (volume 0.37 mL, diameter 6.0 mm) were purchased from Agar Scientific Ltd (Essex, UK). All other chemicals and solvents were of analytical grade or HPLC grade and purchased from Fisher Scientific UK or Sigma-Aldrich, UK. All materials used in the study were within their expiry date when the experimental work was conducted.

2.2. Methods

2.2.1. Dose selection

Dose selection was based on single dose and the water co-administered in the published clinical studies in adults i.e., 50 mg and 100 mg for diclofenac potassium and ritonavir, respectively, administered with 250 mL of water. In experiments with the small-scale systems, the dose was scaled down proportionally to the volume of aqueous media used in the corresponding system (experimental volume), as follows:

$$Scaled\ down\ dose\ (mg) = \frac{Clinical\ dose\ (mg) * experimental\ volume\ (mL)}{250\ mL}$$

As the small-scale two-stage biphasic system has an aqueous volume of 40 mL, the doses tested were 8 and 16 mg for the diclofenac potassium and ritonavir, respectively. For the small-scale two-stage D-P system, the doses were scaled according to the 20 mL donor chamber volume (i.e., 4 and 8 mg for diclofenac potassium and for ritonavir, respectively). The diclofenac potassium and ritonavir tablets were crushed using a pestle and mortar to allow the scale down of the dose required for both small-scale setups. The downsized quantity of formulation then was weighed into a hard gelatine capsule.

2.2.2. Small-scale two-stage biphasic system

The methodology using the inForm (Pion Inc.) instrument was the same as outlined previously (Jankovic et al., 2019; O'Dwyer et al., 2020). Briefly, the relevant quantity of formulation was weighed into a hard gelatine capsule which was added into the system using the automated sample handling mechanism. The test consisted of two stages, representing the transition from gastric to intestinal conditions. The duration of the gastric and intestinal sectors were 30 and 210 min, respectively. Initially the dissolution media consisted of 36 mL of a 0.01 M acetate phosphate buffer at pH 2. After 30 min, 4 mL of ten times concentrated Level II FaSSIF V2 was added into the dissolution vessel and a layer of decanol was added into the vessel. Stirring was temporarily halted and the decanol was added in a dropwise manner to reduce the risk of mixing with the aqueous layer. The pH of the aqueous media was then adjusted to 6.8, to represent the shift into intestinal conditions. The pH transition occurred after addition of the decanol layer to facilitate absorption of drug in the critical period immediately after the shift, where drug substances may be highly supersaturated and liable to

precipitate. pH was controlled to ± 0.1 pH unit of the target pH throughout the experiment by the instrument, adjusting using 0.5 M HCl or 0.5 M NaOH when necessary. Stirring was set to 100 rpm and the temperature was controlled to 37 °C. All experiments were carried out in triplicate. When simulating hypochlorhydric gastric conditions, the pH of the 0.01 M acetate phosphate was set at pH 5 (Litou et al., 2016) during the gastric sector (buffer capacity at pH 5 = 4.8 mEq/pH/L) (Litou et al., 2016; Segregur et al., 2021, 2019). The 0.01 M acetate phosphate buffer was selected as the instrument is calibrated to control the pH using this buffer.

2.2.3. Small-scale two-stage D-P system

The small-scale two-stage D-P system was based on the μFLUX system (Pion Inc.) as outlined previously (O'Dwyer et al., 2020). Briefly, the experiment consisted of two stages to mimic the transition from the stomach to the small intestine. The duration of the gastric and intestinal sectors were 30 and 210 min, respectively. Initially the donor chamber was filled with 15 mL of hydrochloric acid solution (pH 2) and the drug was manually introduced. After 30 min, 5 mL of four times concentrated Level II FaSSIF V2 was added into the donor chamber. The resulting pH in the donor chamber was 6.8 ± 0.1, with further information on the phosphate buffer preparation provided in the Supplementary Materials (table S2). The acceptor chamber was filled throughout the experiment with ASB (20 mL). The two chambers were separated by a biomimetic membrane which consisted of 0.45 μm polyvinylidenfluoride membrane coated with 25 μL of the GIT lipid solution. The surface area of the membrane was 1.54 cm^2. Stirring was provided by cross-bar magnetic stirrers in both chambers and was set at 150 rpm throughout the experiment. All experiments were carried out in triplicate. When simulating hypochlorhydric gastric conditions, the gastric media was a dilute hydrochloric acid solution (pH 5).

2.2.4. Erweka mini-paddle apparatus

Erweka mini-paddle apparatus experiments were carried out using 250 mL volumes in a 500 mL capacity mini-vessel (Erweka) for all media tested. Stirring was set at 75 rpm for each experiment. Formulations were tested in a single medium throughout the experiment i.e., in Level III FaSSGF (fasted state simulated gastric fluid) and in Level II FaSSIF both at 37 °C (Markopoulos et al., 2015). In addition, the ritonavir ASD tablets were tested using Level III hypochlorhydric FaSSGF (Litou et al., 2017). Samples were filtered through a regenerated cellulose 0.45 μm filter (Titan 3, 17 mm, ThermoFisher, MA, USA). Adsorption of drug substances to the filter had been evaluated and found to be negligible in all cases.

2.2.5. BioGIT system

BioGIT system experiments with the diclofenac formulations were performed using the previously outlined methodology (Kourentas et al., 2018). Briefly, the gastric volume was initially filled with 250 mL of Level II FaSSGF in a 500 mL capacity mini vessel (Erweka). The duodenal compartment was initially filled with 40 mL of Level II FaSSIF in a mini vessel with 100 mL capacity from Distek (NJ, USA). The stirring speed was set at 75 rpm in both compartments. Experiments are performed at 37 °C for 45 min using a three-channel peristaltic pump (Reglo ICC pump, part ISM 4308, Ismatec, Wertheim, Germany). To replicate GI transfer, media was pumped from the gastric compartment into the duodenal compartment (flow rate = F1), with media flowing out of the duodenal compartment to replicate the transfer of both undissolved and unabsorbed drug to the lower regions of the small intestine (flow rate = *F*). To maintain both the volume and composition of the fluid in the duodenal compartment throughout the experiment, media from the reservoir compartment was pumped into the duodenal compartment at a flow rate (F2), such that the total flow into the duodenal compartment is identical to flow out of the duodenal compartment ($F = F1 + F2$). The reservoir compartment consisted of a series of phosphate buffer solutions containing sodium chloride, sodium taurocholate, and phosphatidylcholine to keep the composition of simulated duodenal contents constant during the experiment (Kourentas et al., 2018, 2016). Flow rates are changed every 10 min and sampling was performed at the midpoint of these ten-minute intervals, so that emptying of the gastric compartment follows apparent first order kinetics, with a half-life of 15 min. Upon collection, each sample from the duodenal compartment was split into two parts:

- The first part was immediately filtered through 0.45 μm regenerated cellulose filters (Titan 3, 17 mm). This filtrate was then divided into two portions. The first portion was used to determine the dissolved concentration of drug in the duodenal compartment. The second portion of the filtrate was used to estimate the equilibrium solubility of the drug in the medium, by incubating it (37 °C, 75 oscillations/min) in the presence of an excess of solid compound until equilibrium was reached.
- The second part was used to determine the total presence of drug (dissolved and solid drug) in the duodenal compartment. This part was immediately diluted with the mobile phase (without filtration), with the total drug concentration quantified using HPLC, with the HPLC method outlined in Section 2.2.6.

In this study, only experiments with Cataflam® and Voltfast® were performed; BioGIT data for Norvir® have recently been published (Van Den Abeele et al., 2020).

2.2.6. Assay methods

Small-scale two-stage biphasicandD-Psystems: Drug content was quantified primarily using *in situ* fibre optic UV probes. Different standard spectra were collected for the neutral and ionised forms of each compound with the detection wavelengths shown in the supplementary material (Table S3). An excipient in the ritonavir ASD formulation caused significant turbidity in the aqueous media, leading to a high degree of scattering in the UV spectra recorded from the aqueous layer and donor compartments from the small-scale two-stage biphasic and D-P systems, respectively. Due to this scattering present for the ritonavir ASD formulation, it was not possible to quantify drug in these compartments using *in situ* UV probes. However, the decanol layer and acceptor chamber spectra were unaffected by this scattering.

As aqueous concentration data from the small-scale two-stage biphasic system experiment were used to calculate a precipitation rate constant for the PBB model constructed to reflect normal gastric acid rate secretions, offline ultra-performance liquid chromatography (UPLC) quantification methods were used to quantify ritonavir concentrations in the aqueous phase during the experiments performed under conditions assuming normal gastric acid rate conditions. Therefore, samples taken from aqueous layer using the automated liquid handling needle during the first 90 min from the ritonavir biphasic experiments were quantified offline using an Acquity UPLC H—Class Plus (Waters Corporation, MA, USA) with BEH C18 (1.7 μm 2.1 × 50 mm) column using a PDA detector, FTN—H sample manager and a quaternary solvent manager. Data was collected and processed using Empower 3 software (Waters Corporation). The mobile phase comprised a mixture of acetonitrile and 0.1% formic acid (v/v) using a gradient, with further information provided in the supplementary materials (Table S4). The injection volume was 5 μL with a detection wavelength of 254 nm and the limit of quantification (LOQ) was 0.3 μg/mL.

Erweka mini-paddleapparatusand BioGITsystem: Diclofenac samples were quantified using a Dionex UltiMate 3000 HPLC system (Thermo Scientific Inc., MA, USA), with data collected and processed using Chromeleon software (Thermo Scientific Inc.). The mobile phase for diclofenac was ammonium formate pH 3.5 (10 mM): methanol, 25:75 (v/v) with a detection wavelength of 279 nm and LOQ of 0.3 μg/mL. Ritonavir samples were quantified using a Spectra HPLC system consisting of a P1000 pump, an AS1000 autosampler, a UV2000 detector, and an SN4000 controller which was controlled by the Chromquest®

software (version 2.51, Thermo Scientific Inc.). The mobile phase for ritonavir consisted of 0.25% Phosphoric acid: acetonitrile, 45:55 (v/v) and the detection wavelength was 240 nm with a LOQ of 1 μg/mL. Analysis of both drug substances used a Fortis C18 column (3 μm, 150 × 3 mm), a flow rate of 0.5 mL/min and an injection volume was 50 μL.

2.2.7. *Physiologically based biopharmaceutics modelling*

PBB modelling was carried out using the ADAM model which is available as part of the Simcyp simulator (Version 18, Release 2, Certara UK Limited, Sheffield, UK) with the parameters for diclofenac and ritonavir, shown in Tables 1 and 2, respectively. Ten virtual trials using the same number of subjects as the respective clinical studies were simulated in each case and were conducted using the Sim-Healthy Volunteers population in the Simcyp software.

Diclofenac PBB modelling was completed using the stepwise workflow *IVIV*_E (*In Vitro In Vivo* Extrapolation) of solubility and dissolution (Pathak et al., 2019, 2017). Solubility values were estimated using literature data (Guhmann et al., 2013). The diffusion layer model (DLM) scalar was used as part of the dissolution model in the simulator, with the value estimated using the SIVA (Simcyp In Vitro Analysis) software from the dissolution profiles obtained from the Erweka mini-paddle apparatus. A sensitivity analysis was conducted to evaluate the effect of precipitation, if any, on the modelled plasma profile. The transit times of the drug through the GI tract were set at the default mean residence times in the simulator, with a first order gastric emptying process (Hens et al., 2018; Jamei et al., 2009). The distribution of diclofenac was estimated using intravenous (IV) data (Hinz et al., 2005; Willis et al., 1979) and adjusted using the volume of distribution (Davies and Anderson, 1997), via the tissue-plasma partition coefficient (Kp) scalar. Elimination was estimated from IV data (Hinz et al., 2005; Willis et al., 1979).

The biorelevant solubility values were directly inputted into the models for the ritonavir ASD, bypassing the requirement to estimate the micellar: buffer partition coefficients in SIVA. Identifying an appropriate solubility value is challenging for enabling formulations (Litou et al., 2020, 2019). The plateau values from the Erweka mini-paddle apparatus experiments were taken to represent the 'effective' solubility of the formulated drug. The DLM scalar was used as part of the dissolution model, with the value estimated using the SIVA software from the dissolution profiles obtained from the Erweka mini-paddle apparatus. While it is feasible to use small-scale single stage dissolution experiments in the inForm or μDiss platforms to model dissolution, in this instance the data was already available from the Erweka mini-paddle apparatus. Dissolution in the model occurs in the stomach and the intestine of any solid drug, regardless of whether it is undissolved or precipitated drug. An empirical first-order precipitation rate constant (PRC) was estimated by fitting aqueous concentration profiles from the small-scale two-stage biphasic system experiments using Microsoft Excel tools (supplementary materials, Figure S1), as previously outlined (O'Dwyer et al., 2020). Precipitation was considered to have terminated when the drug concentration in the aqueous layer plateaued. Ritonavir was modelled to precipitate to its amorphous state based on previous pH shift dissolution experiments (Miller et al., 2016; Xu et al., 2017). Previous experiments indicated that PRCs estimated from the small-scale two-stage biphasic system were better than those estimated from small-scale two-stage D-P experiments (O'Dwyer et al., 2020). Therefore, the small-scale two-stage D-P system results were not used to estimate precipitation in the PBB model. To simulate hypochlorhydria, the fasted stomach pH in the model was increased to 5.0, with a DLM scalar under hypochlorhydric conditions (Segregur et al., 2021) estimated in the SIVA tool from the hypochlorhydric dissolution profiles obtained from the Erweka mini-paddle apparatus. The transit times of the drug through the GI tract were set at the default mean residence times in the simulator, with a first order gastric emptying process (Hens et al., 2018; Jamei et al., 2009). The volume of distribution was estimated using the physicochemical properties of the molecule, with a Kp scalar employed

Table 1
Values of physicochemical and pharmacokinetic parameters used in the PBB modelling for diclofenac.

Parameter (units)	Values used	References/comments
Physicochemical and blood binding parameters		
Molecular weight (g/mol)	296.15	
Log Po:w	4.4	(Chuasuwan et al., 2009)
Compound type	Monoprotic acid	(Chuasuwan et al., 2009)
pKa	3.8	(Chuasuwan et al., 2009)
Fraction unbound in plasma	0.003	(Accord-UK Ltd, 2018)
Blood plasma ratio	0.7	.(Tang et al., 1999)
Fraction unbound in enterocyte	1	Simcyp compound file
Drug absorption parameters (ADAM model)		
MechPeff Model $P_{trans,0}$ (10^{-6} cm/s)	440,108.3	Predicted using physicochemical properties
Predicted $P_{eff,man}$ ($x10^{-4}$ cm/s)	3.89 (duodenum), 10.06 (jejunum I), 7.05 (jejunum II), 1.65 (Ileum I), 1.65 (Ileum II), 1.62 (Ileum III), 1.56 (Ileum IV), 0.85 (colon)	Predicted in Simcyp using Mechpeff Model
Aqueous intrinsic solubility (mg/mL)	0.0018	Calculated used pH solubility profile (Guhmann et al., 2013)
Solubility factor	546.20	Estimated in Simcyp
Particle density (g/mL)	1.2	Default Simcyp Value
Particle size distribution	Monodispersed	Default Simcyp Value
Particle radius (μm)	10	Default Simcyp Value
Log bile micellar: buffer partition coefficient (Log $K_{m:w}$) neutral	5.91	Estimated in SIVA
Log $K_{m:w}$ ion	0.00038	Estimated in SIVA
Particle diffusion layer thickness (h_{eff}) prediction	Hintz-Johnson method	
Monomer diffusion coefficient (10^{-4} cm^2/min)	4.73	Predicted in Simcyp
Micelle diffusion coefficient (10^{-4} cm^2/min)	0.78	Default Simcyp value
Diffusion layer model (DLM) Scalar (tablet formulation)	31.13	Estimated in SIVA from Erweka mini-paddle dissolution experiment
Disintegration Model	First order	
Maximum% fraction of drug dose dissolved	100	Estimated in SIVA from Erweka mini-paddle dissolution experiment
Kd1	0.17	
Lag (min)	7.43	
Distribution parameters		
Model	Minimal PBPK model	
k_{in} (1/h)	1.88	Estimated using IV data
k_{out} (1/h)	1.48	Estimated using IV data
V_{sac} (L/kg)	0.11	Estimated using IV data
Method	Method 2	
Tissue-plasma partition coefficient (Kp) scalar	2	(Davies and Anderson, 1997)
Steady State Volume of Distribution (Vss) (L/kg)	0.15	Predicted within Simcyp
Elimination parameters		
Intravenous clearance (CL_{iv}) (L/h)	21.50	Estimated using IV data
Renal clearance (L/h)	0.00036	(Rowland and Tozer, 1995)
Population parameters		
Stomach Mean residence time (h)	0.27 (Tablet) / 0.05 (Solution)	

Table 2
Values of physicochemical and pharmacokinetic parameters used in the PBB modelling for ritonavir.

Parameter (units)	Values used	References/comments
Physicochemical and blood binding parameters		
Molecular weight (g/mol)	720.9	
Log Po:w	4.3	In house experimental database
Compound type	Diprotic Base	In house experimental database
pKa	1.8, 2.6	In house experimental database
Fraction unbound in plasma	0.005	(Denissen et al., 1997)
Blood plasma ratio	0.66	Predicted in Simcyp
Fraction unbound in enterocyte	1	Simcyp compound file
Drug absorption parameters (ADAM Model)		
MechPeff Model $P_{trans,0}$ (10^{-6} cm/s)	1465.85	Predicted using physicochemical properties
Predicted $P_{eff,man}$ ($x10^{-4}$ cm/s)	2.84 (duodenum), 7.56 (jejunum I), 5.30 (jejunum II), 1.15 (Ileum I), 1.15 (Ileum II), 1.13 (Ileum III), 1.09 (Ileum IV), 0.59 (colon)	Predicted in Simcyp using Mechpeff Model
Aqueous intrinsic solubility (mg/mL)	0.061	Calculated using intestinal dissolution plateau values from the Erweka mini-paddle apparatus (this study)
Solubility factor	4.25	Estimated using the maximum concentrations observed in Erweka mini-paddle dissolution experiments
Particle density (g/mL)	1.2	Default Simcyp value
Particle size distribution	Monodispersed	Default Simcyp value
Particle radius (μm)	10	Default Simcyp value
Particle h_{eff} prediction	Hintz-Johnson method	
Critical supersaturation ratio	1.00	Calculated from kinetic solubility data from solvent shift experiments (see Section 3.2.4) and (Xu et al., 2017)
Precipitation rate constant (PRC) (1/h)	9.45	Calculated from biphasic experimental data. Note precipitation to amorphous state (Miller et al., 2016; Xu et al., 2017).
Monomer diffusion coefficient (10^{-4} cm^2/min)	3.14	Predicted in Simcyp
Micelle diffusion coefficient (10^{-4} cm^2/min)	0.78	Default Simcyp value
DLM Scalar	0.028 (stomach), 0.016 (hypochlorhydric stomach), 0.072 (intestine)	Estimated in SIVA from Erweka mini-paddle dissolution experiment. Note dissolution occurs of any solid drug, irrespective of origination as undissolved or precipitated drug
Distribution parameters		
Model	Full PBPK model	
Method	Method 2	
Kp scalar	0.06	(Hsu et al., 1998)
Vss (L/kg)	0.35	Predicted within Simcyp
Elimination parameters		
CYP2D6	0.7 (Vmax), 1.0 (Km)	Simcyp compound file
CYP3A4	1.37 (Vmax), 0.07 (Km)	Simcyp compound file with BD SUP ISEF (Intersystem extrapolation factor)
CYP3A5	1.0 (Vmax) 0.05 (Km)	Simcyp compound file with BD SUP ISEF
Renal clearance (L/h)	0.006	(Rowland and Tozer, 1995)

to adjust the volume of distribution. Elimination parameters were modelled using enzyme kinetic studies (Koudriakova et al., 1998) using information provided as part of the "SV-Ritonavir" compound default file in the simulator.

The Fold Difference (FD) ratio of the predicted vs. observed parameters, i.e., area under the plasma concentration-time curve (AUC), maximum plasma concentration (C_{max}), and time to reach C_{max} (T_{max}) were used to evaluate the modelled results. In addition, the absolute average fold error (AAFE) (Eq. (1)) was calculated (Andreas et al., 2017; Poulin and Theil, 2009) to evaluate the modelled mean plasma profiles. *n* is the number of time points at which the concentration was determined, with *predicted i* and *observed i* being the predicted and observed concentrations at a given time point i. AAFE shows the absolute error of the simulation compared to the observed profiles, with values of < 2 considered to show a successful simulation.

$$AAFE = 10^{\left(\frac{1}{n}\right)*\sum\left|Log\left(\frac{predicted\ i}{observed\ i}\right)\right|} \quad (1)$$

2.2.8. Extraction of published in vivo data

Previously published *in vivo* data for diclofenac (Marzo et al., 2000; Van Den Abeele et al., 2017) and ritonavir (Ng et al., 2008; Van Den Abeele et al., 2020) were extracted using WebPlotDigitizer (version 4.2, WebPlotDigitizer, CA, USA).

3. Results and discussion

3.1. Diclofenac

3.1.1. Small-scale two-stage biphasic system

Initially both formulations appeared to be transiently highly supersaturated in the gastric sector, before precipitation of both formulations was subsequently observed (Fig. 1). Despite this precipitation, the powder formulation had a higher concentration of diclofenac in solution compared to the tablet formulation at the end of the testing period in the gastric sector; mean ± SD ($n = 3$) values were 8.48 ± 0.43 and 2.03 ± 0.21% (w/w) of the dose for the powder and the tablet formulation, respectively. In particular, the powder formulation appeared to be supersaturated compared to the equilibrium concentration of the free acid in dilute HCl (Guhmann et al., 2013) of approx. 1.3% (converted to an equivalent percentage (w/w) of the dose), indicating a solubilising effect of the formulation's excipients (Wisdom Pharmaceutical Technology Co Limited, 2020). However, an in-depth study of the solubilising effect of each excipient in the formulation was beyond the scope of this work.

Upon the switch to intestinal conditions, the drug substance from both formulations was rapidly dissolved in the aqueous layer and the drug readily partitioned into the decanol layer. Interestingly, the ionisation of diclofenac in the intestinal sector did not prevent partitioning into the decanol layer, with more than 85% (w/w) of the dose in solution in the decanol layer for both formulations at the end of the experiment. The results from both layers indicated that both formulations would dissolve rapidly upon entry into the upper small intestine and that a similar AUC should be achieved by both formulations, correlating with the observed $AUC_{0-\infty}$ from the clinical study (Marzo et al., 2000). However, the more rapid C_{max} and greater $AUC_{0-2\ h}$ observed for the powder formulation in the clinical study was not highlighted by the

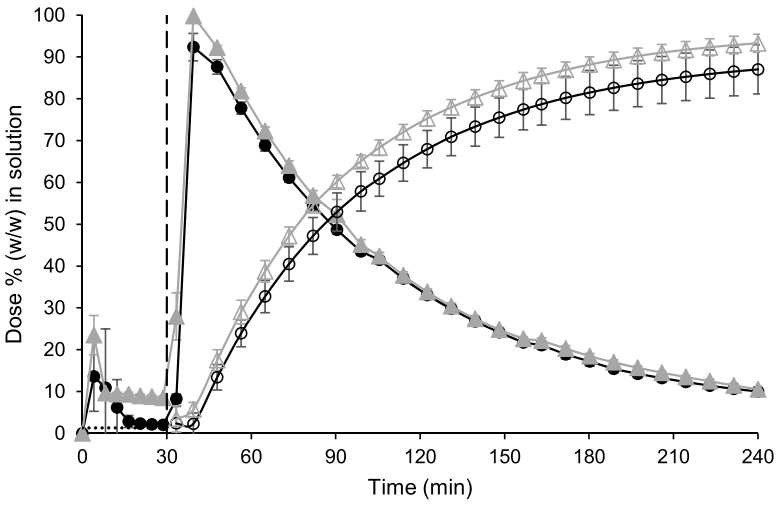

Fig. 1. Mean ± SD (n = 3) diclofenac data from the small-scale two-stage biphasic system experiments. Percentage of dose (w/w) in solution in the aqueous and decanol layers are represented by the filled and hollow symbols, respectively. Cataflam® and Voltfast® data are represented by black circles and grey triangles, respectively. The dashed line indicates the time of transition from simulated gastric to simulated intestinal conditions. The horizontal dotted line corresponds to the equilibrium concentration of the free acid in dilute HCl (Guhmann et al., 2013) (converted to an equivalent percentage (w/w) of the dose).

small-scale two-stage biphasic system results, with similar concentration-time profiles recorded for both formulations using the setup (Fig. 1).

3.1.2. Small scale two-stage D-P system

Similar to the small-scale two-stage biphasic system experiments, both formulations were initially highly supersaturated in the gastric sector in the donor chamber with the greatest mean ± SD (n = 3) values measured concentration in the gastric sector of 13.88 ± 0.98 and 6.27 ± 1.10 μg/mL for the powder and the tablet formulation, respectively, compared to the reported solubility of 2.49 μg/mL in dilute HCl (Guhmann et al., 2013). For both formulations, precipitation subsequently occurredin the donor chamber during the gastric sector (Fig. 2a). At the end of the gastric sector, the concentration of the powder formulation was higher than the tablet formulation in the donor chamber; mean ± SD (n = 3) values were 4.25 ± 0.80 and 1.08 ± 0.13% (w/w) of the dose for powder and tablet formulation, respectively. The powder formulation appeared to be supersaturated compared to the equilibrium concentration of the free acid in dilute HCl (Guhmann et al., 2013) of approx. 1.1% (converted to an equivalent percentage (w/w) of the dose). While these concentrations in donor chamber at the end of the gastric sector are lower than the equivalent concentrations in the small-scale two-stage biphasic system, the membrane in the small scale two-stage D-P system is *in situ* throughout the experiment allowing 'absorption' of drug into the acceptor chamber during the gastric sector, unlike the small-scale two-stage biphasic system.

Upon transition to intestinal conditions, the donor chamber concentrations indicated that both formulations would rapidly dissolve. The powder formulation was more rapidly dissolved compared to the tablet formulation, correlating with the more rapid C_{max} observed for the powder formulation in the clinical study (Marzo et al., 2000), unlike the small-scale two-stage biphasic system experiments which showed a minimal difference between formulations (Fig. 1).

The concentration in the acceptor chamber for the tablet (Fig. 2b) was lower than the powder formulation throughout the experiment, with mean ± SD (n = 3) values at the end of the experiment of 3.33 ± 0.53 and 5.25 ± 0.50% (w/w) of the dose for the tablet and powder formulation, respectively. Most of the difference in acceptor chamber

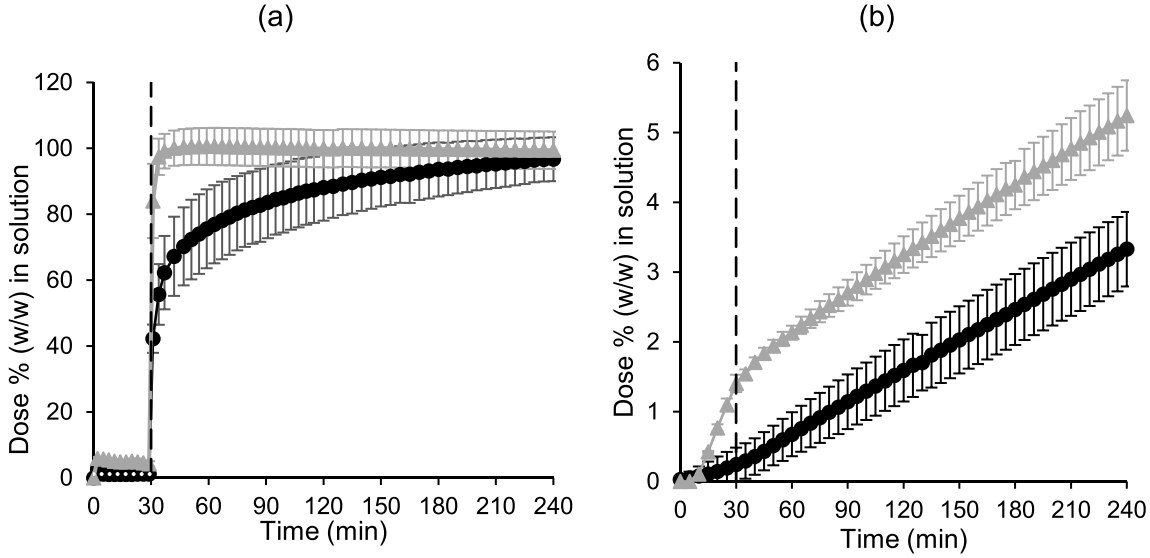

Fig. 2. Mean ± SD (n = 3) diclofenac data from the small-scale two-stage D-P system experiments. (a) Percentage of dose (w/w) in solution in the donor chamber; (b) Percentage of dose (w/w) in solution in the acceptor chamber. The dashed line indicates the time of transition from simulated gastric to simulated intestinal conditions. Cataflam® and Voltfast® data are represented by black circles and grey triangles, respectively. The horizontal dotted line corresponds to the equilibrium concentration of the free acid in dilute HCl (Guhmann et al., 2013) (converted to an equivalent percentage (w/w) of the dose).

concentrations between formulations (1.16% (w/w) of the dose) was due to flux of drug into the acceptor chamber during the gastric sector. The predominantly nonionised drug could readily pass through the membrane during the gastric sector, as the membrane was *in situ* throughout the experiment. This feature of the setup could be useful to simulate possible gastric absorption, if any, which may partly account for the greater C_{max} observed for the powder formulation. While there is some evidence for gastric absorption of diclofenac in rats (Rubbens et al., 2018) and humans (Vidon et al., 1989), this discussion regarding the significance of gastric absorption is highly contentious and beyond the scope of this study.

A disadvantage of both small-scale systems is that any variance due to differences in gastric emptying times between the formulations cannot be detected, as the switch from gastric to intestinal conditions occurs at a single time point in both systems. Another disadvantage of using small-scale methods is the requirement to crush the dosage form to scale-down the dose. While the rupture time of the gelatine capsules will somewhat replicate the disintegration time of the tablet, the effect of disintegration as differentiator between the formulations is overlooked.

3.1.3. Erweka mini-paddle apparatus

In Level III FaSSGF, both formulations supersaturated in the dissolution medium for a few minutes, followed by precipitation of the free acid down to the equilibrium solubility (Fig. 3a) (Guhmann et al., 2013). Rapid and complete (> 95%) diclofenac dissolution from both formulations was observed in Level II biorelevant intestinal media (Fig. 3b). The effect of disintegration on the formulations was clearly observed with a delayed release of drug from the tablet formulation. In contrast, dissolution from the powder formulation was very rapid with > 95% of the dose in solution by the first time point after 5 min (Fig. 3b).

3.1.4. BioGIT system

The tablet formulation had a 14.5% smaller $AUC_{Duodenal,\ 0\ -\ 0.75\ h}$ compared to the powder formulation (33.50 vs. 39.19 μg. h/mL, $n = 3$) using the BioGIT system (Fig. 4). For both formulations, no solid drug was detected in the intestinal chamber, due to the high solubility of diclofenac in an intestinal environment. This matched behaviour observed in the duodenal aspirates of healthy volunteers, after administration of the tablet formulation in the fasting state (Van Den Abeele et al., 2017, 2016). Unfortunately, intraluminal concentrations after administration of the powder formulation are not available.

The clinical study in healthy adults has shown that the tablet formulation had a 35% smaller $AUC_{Systemic,\ 0–2\ h}$ than the powder formulation (Marzo et al., 2000), with the powder formulation also having an earlier median t_{max} than the tablet formulation (0.25 vs. 0.63 h). This difference in early exposure between the formulations was successfully simulated by the BioGIT system data on a qualitative basis; the mean $AUC_{Duodenal,\ 0–0.75\ h}$ value estimated from concentration vs. time BioGIT system data for the tablet formulation was lower than the corresponding value for the powder formulation. Although BioGIT system has not been designed to capture physiological differences in gastric emptying rates between formulations, especially when the *in vivo* data are highly variable as evidenced from the gastric and duodenal aspirate samples (Van Den Abeele et al., 2017, 2016), BioGIT system diclofenac data collected in this study may contribute to understanding the relationship of BioGIT system data with human data on a quantitative basis (Kourentas et al., 2018).

3.1.5. Physiologically based biopharmaceutics modelling

PBB modelling for the tablet formulation using the DLM scalar and disintegration parameters, both estimated from the Erweka mini-paddle apparatus data, resulted in a good fit (AAFE = 1.55) relative to the previously observed average plasma profile in adults (Fig. 5a, Table 3). The simulated duodenal concentrations showed complete dissolution of the tablet formulation in the model, analogous to the BioGIT system data. The modelled duodenal concentrations for both diclofenac formulations are in-line with the concentrations in the BioGIT duodenal compartment (Fig. 4).

As the powder for oral solution is pre-dissolved in a glass of water prior to administration, it was treated as an oral solution in the model. This model for the powder formulation indicated that the key parameters for modelling the rate of oral absorption for diclofenac were the gastric residence time in the simulated population and the permeability of drug in the upper small intestine. In an attempt to replicate this rapid early exposure of the powder formulation, the mean residence time in the stomach was reduced from the default of 0.36 to 0.05 h. Despite this reduced gastric residence time, the modelled T_{max} was later with a smaller C_{max} compared to the clinical results (Fig. 5b, Table 3), which indicated that permeability in the upper small intestine was underestimated in the model. A sensitivity analysis was carried out examining

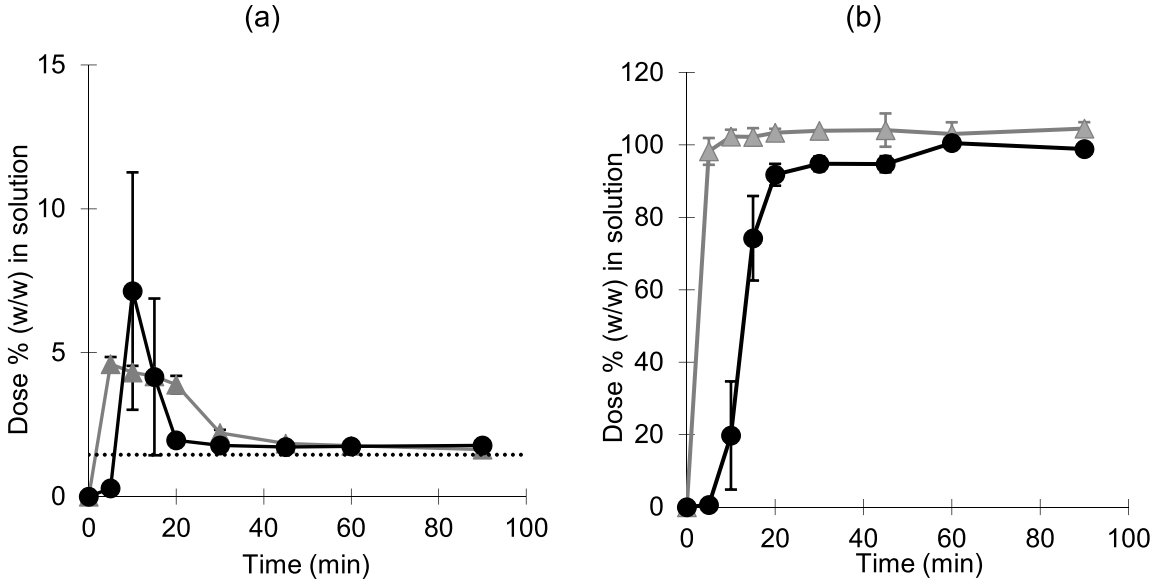

Fig. 3. Mean ± SD ($n = 3$) percentage diclofenac dissolved (w/w) when using the Erweka mini-paddle apparatus (75 rpm) in 250 mL Level III FaSSGF (a) and in 250 mL Level II FaSSIF (b). Cataflam® and Voltfast® data are represented by black circles and grey triangles, respectively. The horizontal dotted line corresponds to the equilibrium concentration of the free acid (converted to an equivalent percentage (w/w) of the dose).

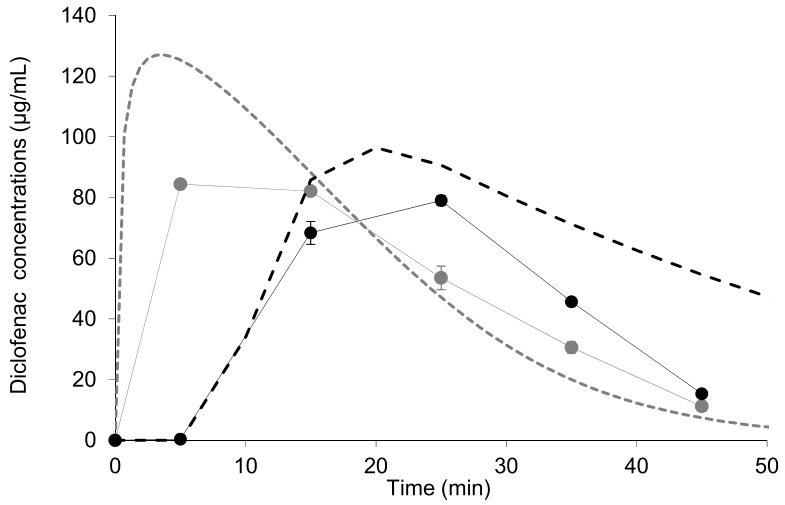

Fig. 4. Mean ± SD (n = 3) apparent diclofenac concentrations in the duodenal compartment of BioGIT (circles) and simulated duodenal profiles using PBB modelling (dashed line) for Cataflam® (grey) and Voltfast® (black).

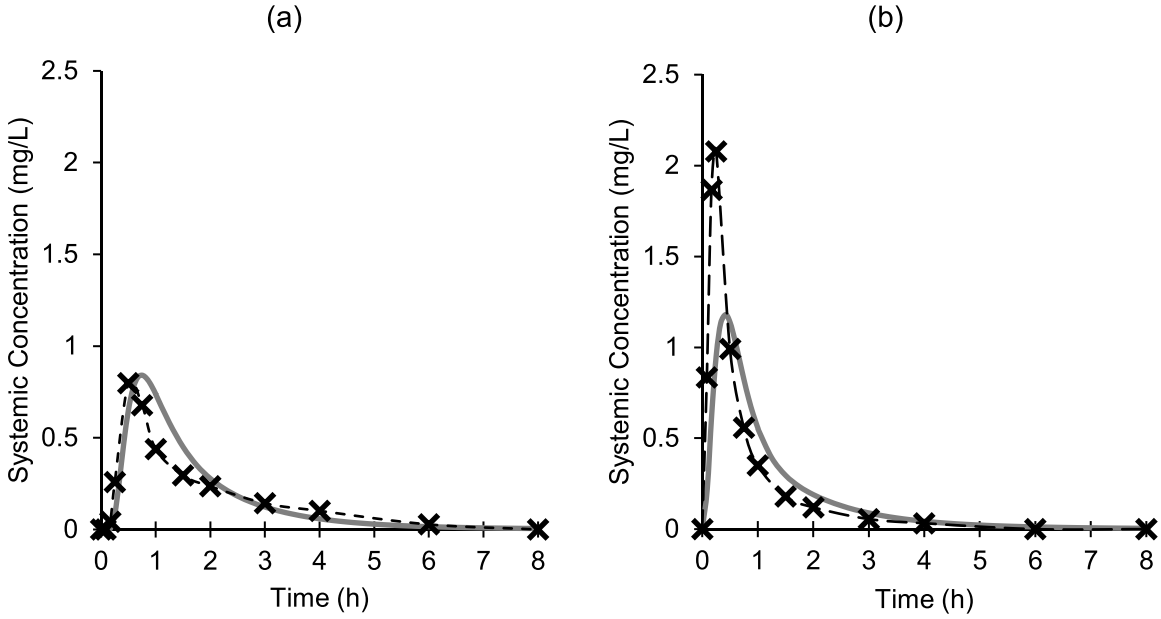

Fig. 5. Mean diclofenac plasma concentrations after single oral administration of Cataflam® (a) and Voltfast® (b) to healthy adults in the fasted state (-x-); measures of variability were not reported in the relevant reference (Marzo et al., 2000). Continuous lines are simulated plasma profiles using PBB modelling.

Table 3
Values of pharmacokinetic parameters calculated from in vivo data (n = 24) (Marzo et al., 2000) and estimated using PBB modelling (this study) for Cataflam® and Voltfast*.

	Cataflam®				Voltfast®			
	***In vivo* data**	**PBB model**	**FD**	**AAFE**	***In vivo* data**	**PBB model**	**FD**	**AAFE**
Mean AUC (µg.h/mL)	1.21	1.32	1.09	1.55	1.36	1.38	1.01	1.80
Mean C_{max} (mg/L)	1.07	0.93	0.87		2.21	1.19	0.54	
Median T_{max} (h)	0.63	0.76	0.86		0.25	0.41	1.80	

AAFE: Absolute Average Fold Error; FD: fold difference predicted/observed.

the effect of intestinal permeability on the simulated plasma profile in the model, showing an earlier T_{max} and increased C_{max} with increasing intestinal permeability values (Supplementary Material, Figure S2).

While it is unlikely that intestinal permeability varied significantly between the formulations, it appears the rate limiting step of drug absorption was different between the formulations. The absorption of drug from the tablet appeared to be delayed due to disintegration, while absorption of drug from the powder for oral solution was primarily dependant on gastric emptying and/or the intestinal permeability of the drug. For both formulations, the models were not sensitive to precipitation in the stomach as any solid drug was rapidly dissolved in the intestine, due to its high solubility in intestinal conditions.

3.2. Ritonavir

3.2.1. Small-scale two-stage biphasic system

Rapid precipitation of the drug was observed upon transfer from gastric to intestinal conditions in the experiment simulating normal gastric conditions (Fig. 6). The precipitation rate constant calculated from this experiment was incorporated into a PBB model, as outlined in Section 2.2.7. Similar concentrations were observed in the decanol layer using both normal and hypochlorhydric gastric conditions. This correlates nicely with the information provided in the summary of product characteristics (SmPC), which indicates that concurrent administration of a proton pump inhibitor (PPI) or H_2 antagonist did not affect the efficacy of ritonavir, with only a small decrease in drug exposure (AbbVie Deutschland GmbH & Co. KG., 2016). In addition, duodenal aspirates from fasted healthy volunteers showed no significant change in ritonavir concentration after administration with esomeprazole (Van Den Abeele et al., 2020). As the small-scale two-stage biphasic system only accounts for the changes in gastric pH caused by the PPI, it does not simulate any other physiological effects caused by the PPI which may affect systemic concentrations (Babaei et al., 2009; de Waal et al., 2020; Segregur et al., 2019; Van Den Abeele et al., 2020).

3.2.2. Small-scale two-stage D-P system

Profiles in the acceptor compartment suggest no significant impact of hypochlorhydric conditions to the absorption of ritonavir from the ASD product (Fig. 7), in-line with the *in vivo* observations (AbbVie Deutschland GmbH & Co. KG., 2016; Morcos et al., 2014; Van Den Abeele et al., 2020). Analogous to the small-scale two-stage biphasic system experiments, this hypochlorhydric setup only accounts for changes in the gastric pH caused by the PPI.

3.2.3. Erweka mini-paddle apparatus

Using the Erweka mini-paddle apparatus, there was a higher percentage of the dose in solution in Level III FaSSGF at a normal gastric pH compared to the hypochlorhydric conditions; mean ± SD ($n = 3$) values were 67.59 ± 1.76 and 7.67 ± 0.06% (w/w) of the dose under normal and reduced gastric acid conditions, respectively (Fig. 8). However, the clinical study showed that concentrations of drug in the duodenum were not significantly affected by the hypochlorhydric gastric conditions (AbbVie Deutschland GmbH & Co. KG., 2016; Morcos et al., 2014; Van Den Abeele et al., 2020). These results highlighted the necessity to incorporate the GI transfer process as part of the *in vitro* testing, to improve the understanding of the behaviour of this ritonavir ASD. Dissolution data from the Erweka mini-paddle apparatus experiments were incorporated into an PBB model and are discussed in parallel with the data from the small-scale two-stage biphasic system in Section 3.2.4.

3.2.4. Physiologically based biopharmaceutics modelling

Initially, modelling was completed using the default DLM scalar (i.e., DLM = 1) without incorporating precipitation to evaluate if a decent model could be established without including experimentally derived values for either precipitation or dissolution in the model. This model produced a poor fit relative to the *in vivo* profile (AAFE = 3.52), with a very large overestimation of both AUC and C_{max} (Table 4). This highlighted that experimentally determined values for the dynamic dissolution process are vital to incorporate into the model. Therefore, the impact of the dynamic dissolution process, incorporating dissolution and precipitation of drug (McAllister, 2010), on the oral absorption of ritonavir from Norvir® was investigated.

The effects of including experimentally determined values for dissolution and precipitation were first examined individually in the model to improve the understanding of the sensitivity of the parameters in the model. Thus, the dissolution results from the Erweka mini-paddle apparatus dissolution results simulating both gastric and intestinal conditions (Section 3.2.3) were included in the model without precipitation present. The dissolution rate was incorporated into the model via the DLM scalar, estimated in SIVA from the Erweka mini-paddle apparatus dissolution results. This model resulted in an overestimation of both C_{max} and AUC (Fig. 9, Table 4, AAFE 1.50), highlighting that slow and/or incomplete dissolution was not the sole limiting factor for the oral absorption of the ritonavir from Norvir®.

The effect of precipitation on oral absorption was then examined. Previous studies have shown that the small-scale two-stage biphasic system was a suitable *in vitro* method to calculate the PRC of a weakly basic drug, as it transitions from gastric to intestinal conditions (O'Dwyer et al., 2020). Using the biphasic results, a high PRC was calculated of 9.45 h^{-1} indicating a very rapid precipitation of drug upon entry into the intestine. The critical supersaturation ratio (CSR) was 1, as the critical supersaturation concentration determined from solvent shift experiments of ritonavir using Level II intestinal media (35.96 μg/mL) was below the observed kinetic solubility of ritonavir from Norvir® in Level II intestinal media (Xu et al., 2017). This effect was potentially due to the sorbitan laurate in the formulation (AbbVie Deutschland GmbH & Co. KG., 2016), which is believed to alter the precipitation and crystallisation behaviour of drugs (Chen et al., 2017).

Simulations using the PRC calculated from the small-scale two-stage

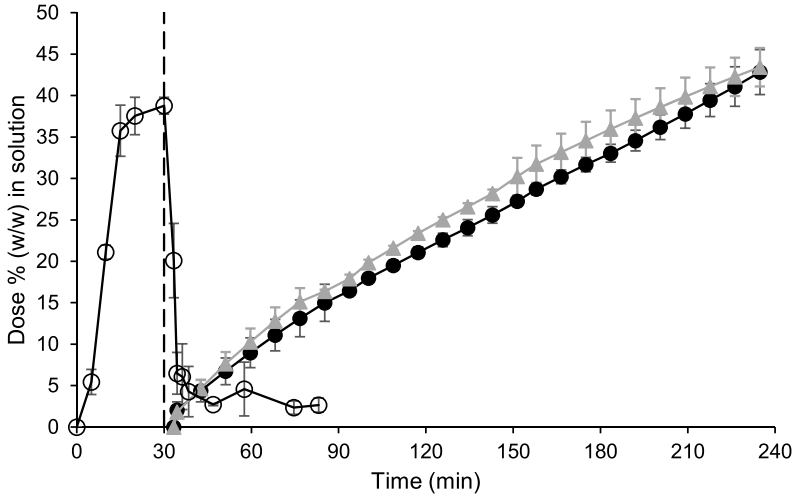

Fig. 6. Mean ± SD ($n = 3$) ritonavir data from the small-scale two-stage biphasic system experiments. Percentage of dose (w/w) in solution in the aqueous and decanol layers are represented by the filled and hollow symbols, respectively. Simulated normal gastric and hypochlorhydric conditions are represented by black circles and grey triangles, respectively. The dashed line indicates the time of transition from simulated gastric to simulated intestinal conditions.

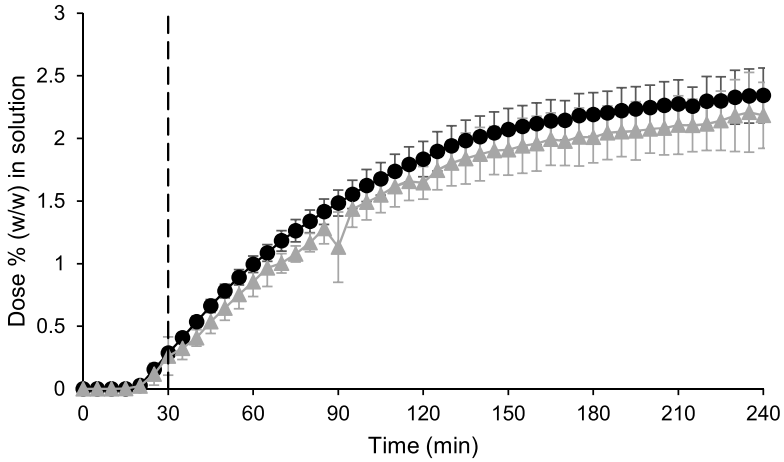

Fig. 7. Mean ± SD ($n = 3$) percentage of ritonavir (w/w) in solution in the acceptor chamber of the small-scale two-stage D-P system. The dashed line indicates the time of transition from simulated gastric to simulated intestinal conditions. Simulated normal and hypochlorhydric gastric conditions are represented by black circles and grey triangles, respectively.

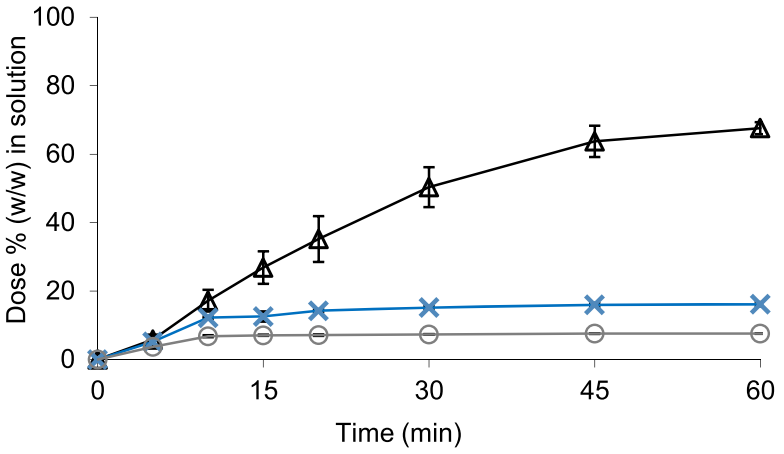

Fig. 8. Mean ± SD ($n = 3$) percentage of ritonavir dissolved (w/w) from Norvir® in 250 mL Level III FaSSGF (Δ), 250 mL Level III hypochlorhydric FaSSGF (○), and 250 mL Level II FaSSIF (x) when using the Erweka mini-paddle apparatus (75 rpm).

Table 4
Values of pharmacokinetic parameters calculated from in vivo data ($n = 27$) (Ng et al., 2008) and estimated using PBB modelling (this study) for Norvir® 100 mg tablets.

	***In vivo* data**	**Default DLM scalar value & no precipitation**			**Experimentally derived DLM scalar value (no precipitation)**			**Experimentally derived PRC value (default DLM scalar value)**			**Experimentally derived PRC and DLM scalar values**			**Hypochlorhydric gastric conditions**		
		PBB model	**FD**	**AAFE**	**PBB model**	**FD**	**AAFE**	**PBB model**	**FD**	**AAFE**	**PBB model**	**FD**	**AAFE**	**PBB model**	**FD**	**AAFE**
Mean AUC (μg.h/mL)	4.7	14.45	3.07	3.52	6.29	1.34	1.50	5.71	1.22	1.37	4.76	1.01	1.26	4.43	0.94	N/A
Mean C_{max} (mg/L)	0.60	2.07	3.44		0.74	1.24		0.68	1.13		0.56	0.93		0.52	0.87	
Mean T_{max} (h)	3.2	1.06	0.33		1.53	0.48		2.19	0.68		2.16	0.68		2.35	0.73	

AAFE: Absolute Average Fold Error; FD: fold difference predicted/observed; PRC = Precipitation Rate Constant; DLM = Diffusion Layer Model.

biphasic system experiments were carried out employing the default DLM scalar value (i.e., DLM = 1) in the model, to examine whether precipitation alone was the key limiting factor for the oral absorption of the ritonavir ASD formulation. Modelling using the default DLM scalar resulted in an overestimation of the AUC and C_{max} compared to the clinical results (Fig. 9, Table 4, AAFE 1.37), indicating that precipitation alone did not fully account as the limiting factor for drug absorption. Therefore, the effect of dissolution and precipitation together on oral absorption was examined.

Using DLM scalar values and a precipitation rate estimated from the Erweka mini-paddle apparatus and the small-scale two-stage biphasic system experiments, respectively, improved the performance of the model relative to the previously published plasma data in adults (Fig. 9). The modelled AUC and C_{max} using the 'combined' model had a smaller

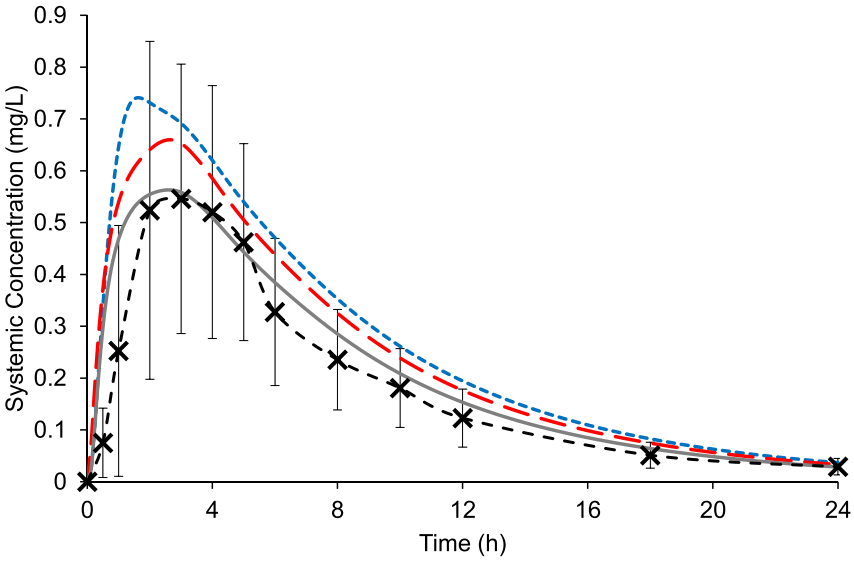

Fig. 9. Mean (± SD) ritonavir plasma concentrations after single dose administrations of one Norvir® tablet to fasted healthy adults (Ng et al., 2008) vs. simulated ritonavir plasma profiles using PBB modelling and the experimentally determined DLM scalar value (no precipitation) i.e., using the Erweka mini-paddle apparatus data (blue dotted line), the experimentally determined PRC & default DLM scalar value i.e.,. the small-scale two-stage biphasic system data (red dashed line), and the experimentally determined PRC & DLM scalar values i.e., using both Erweka mini-paddle apparatus and small-scale two-stage biphasic system data (solid grey line). (For interpretation of the references to colour in this figure legend, the reader is referred to the web version of this article.)

prediction error (PE) relative to the *in vivo* results compared to the other modelled profiles (Table 4) with the smallest AAFE of 1.26. Therefore, both dissolution and precipitation parameters were necessary for building an adequate model for Norvir®. While keeping in mind any limitations or uncertainties regarding modelling, this highlights the benefit of combining PBB modelling with biorelevant *in vitro* testing as part of the drug formulation development process, even after clinical testing, as modelling can be a source of additional valuable insight. In this study, the modelling after the clinical study improved the understanding of the factors limiting oral absorption which were not directly apparent from the clinical study results alone. Furthermore, the modelled duodenal concentrations under normal gastric conditions are in-line with the concentrations in the BioGIT duodenal compartment (Van Den Abeele et al., 2020) (Fig. 10a).

The model under hypochlorhydric conditions in the stomach, resulted in a minor decrease in the AUC and C_{max} (Table 4), in-line with the range provided in the summary of product characteristics (6 – 18%) for Norvir (AbbVie Deutschland GmbH & Co. KG., 2016) and results from a clinical study (n = 13), where the effects of co-administration of ranitidine or omeprazole on the pharmacokinetics of danoprevir/ritonavir were examined (Morcos et al., 2014). The modelled duodenal concentrations under hypochlorhydric conditions appear to be lower than the concentrations BioGIT duodenal compartment (Van Den Abeele et al., 2020) (Fig. 10b) which may be due to an underestimation of the DLM scalar under hypochlorhydric conditions. However, due to the large variability observed among in vivo duodenal concentrations, uncertainty remains regarding ritonavir's behaviour in this initial period post administration. In any case, early duodenal exposure in the initial 45 min is unlikely to be the critical factor in ritonavir absorption considering the reported C_{max} and plasma half-life of ritonavir of 3.2h and 5.5 h, respectively (Ng et al., 2008). Plasma profiles from the Van den Abeele et al. study examining the effect of pre-treatment with a PPI were inconclusive, due to the extremely large variability observed between the healthy volunteers, potentially related to the small number of participated volunteers (n = 5) (Van Den Abeele et al., 2020). In addition, the authors deduced that physiological effects of the PPI other than the impact on gastric pH, such as a change in GI fluid volumes (Segregur et al., 2019), may have impacted the systemic plasma profiles (de Waal

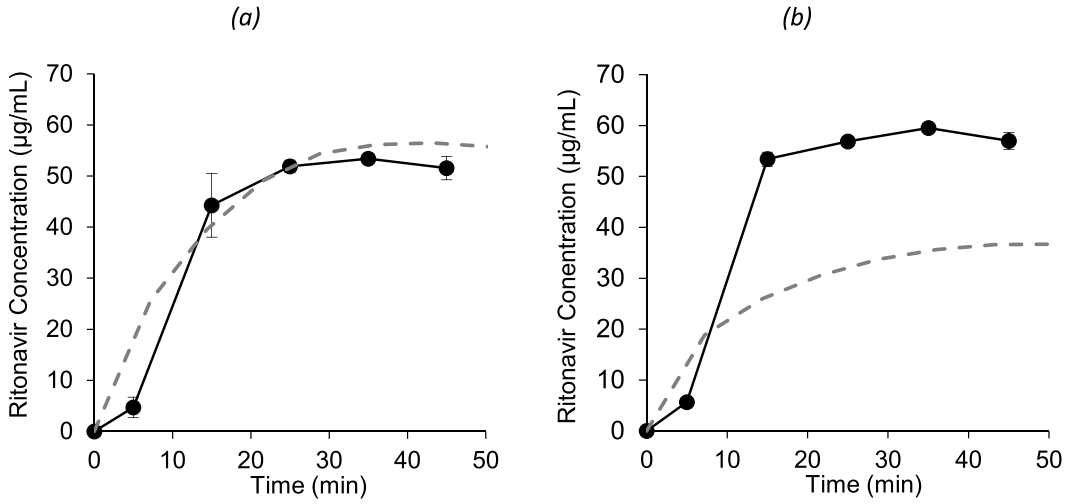

Fig. 10. Mean ± SD (n = 3) apparent ritonavir concentrations in the duodenal compartment of BioGIT (-•-) (reproduced from Van Den Abeele et al. 2020) and simulated ritonavir duodenal profiles using PBB modelling (- - -) assuming that one Norvir® tablet is administered under normal (a) and hypochlorhydric (b) gastric conditions.

et al., 2020; Van Den Abeele et al., 2020). The choice of PPI selected for co-administration with ritonavir may be a significant factor with less pronounced effects on gastric volumes associated with omeprazole compared to other PPIs (Gursoy et al., 2008). As the PBB model presented in this study only simulated the effect on the gastric pH caused by the PPI, it would overlook any of these potential physiological effects of the PPI. With further understanding of the complete physiological effects of the PPIs, improved PBB models could be designed to predict the effect of PPI pre-treatment.

4. Concluding remarks

This study indicates that selection of the appropriate *in vitro* method for evaluating the intraluminal performance of poorly soluble, ionisable drugs depends primarily on the characteristics of the drug substance.

For the diclofenac potassium formulations, the Erweka mini-paddle apparatus results in Level II biorelevant media alone were sufficient to capture the effects, if any, on *in vivo* dissolution. For drugs such as diclofenac, the issue of availability and ease of operation of the *in vitro* system are the key points of consideration.

For Norvir®, detailed information on its behaviour both under gastric simulated conditions and under conditions simulating those in the upper small intestine was crucial for understanding the luminal performance. An improved PBB model was created by incorporating both dissolution and precipitation parameters into the model using results from both the Erweka mini-paddle apparatus and the small-scale two-stage biphasic system experiments, respectively. Simulation of the gastrointestinal transfer process from the stomach to the small intestine was necessary to evaluate the effects of hypochlorhydric conditions on the luminal performance of the ritonavir ASD.

Using *in situ* UV dip probes to quantify drug in both small-scale setups facilitated a rapid throughput of experiments, by avoiding off-line quantification steps. The advantage of small-scale two-stage biphasic system was the more rapid absorption of drug in the intestinal conditions compared to the small-scale two-stage D-P system. In addition, the small-scale two-stage biphasic system allowed the flexibility to introduce the absorption sink as determined by the user, whereas the absorption sink is in place throughout the small-scale two-stage D-P system experiments. On the other hand, the setup of the small-scale two-stage D-P system platform allowed the triplicate experiments to be in parallel, facilitating a more rapid throughput than the small-scale two-stage biphasic system. Furthermore, the small-scale two-stage D-P system experiments have a smaller operating volume (20 mL) than the small-scale two-stage biphasic system (40 mL), allowing for a reduced quantity of drug employed in these experiments. The Erweka mini-paddle apparatus experiments are less complex to operate than the BioGIT system and can be run in parallel. However, the BioGIT system is useful to provide information about the dynamic behaviour of the drug in the duodenum.

Regardless of the type of the drug substances, early in the drug development process, when availability of drug amounts and/or dose units is limited, the Erweka mini-paddle apparatus or the BioGIT system [at least if not at its mini-version (https://pergamos.lib.uoa.gr/uoa/dl/frontend/file/lib/default/data/2775881/theFile)] may not be applicable. Therefore, small-scale systems are necessary at this stage. This study examined the application of the small-scale systems to comparatively assess performance of formulations in the GI tract and to obtain parameters for PBB modelling. However, other applications of these small-scale systems are potentially possible, such as directly obtaining a quantitative estimation of oral absorption in early development, and are worthy of further investigation in future studies. When applying small-scale setups, it is important to be mindful of limitations associated with the respective setups, such as the necessity to crush the dosage forms, when interpreting the data. At later stages of development, full-scale methods should be employed.

CRediT authorship contribution statement

Patrick J O'Dwyer: Data curation, Formal analysis, Investigation, Methodology, Software, Writing – original draft, Writing – review & editing. **Karl J Box:** Funding acquisition, Methodology, Project administration, Writing – review & editing. **Georgios Imanidis:** Data curation, Writing – review & editing. **Maria Vertzoni:** Conceptualization, Data curation, Writing – review & editing. **Christos Reppas:** Conceptualization, Funding acquisition, Data curation, Investigation, Methodology, Project administration, Supervision, Visualization, Writing – review & editing.

Acknowledgments

This work was supported by the European Union's Horizon 2020 Research and Innovation Programme under grant agreement No 674909 (PEARRL).

Supplementary materials

Supplementary material associated with this article can be found, in the online version, at doi:10.1016/j.ejps.2021.106034.

References

AbbVie Deutschland GmbH & Co. KG., 2016. Norvir 100 mg tablets. Summary of Product Characteristics.

Accord-UK Ltd, 2018. Diclofenac Potassium 50 mg Tablets. Summary of Product Characteristics.

Andreas, C.J., Pepin, X., Markopoulos, C., Vertzoni, M., Reppas, C., Dressman, J.B., 2017. European Journal of Pharmaceutical Sciences Mechanistic investigation of the negative food effect of modified release zolpidem. Eur. J. Pharm. Sci. 102, 284–298. https://doi.org/10.1016/j.ejps.2017.03.011.

Babaei, A., Bhargava, V., Aalam, S., Scadeng, M., Mittal, R.K., 2009. Effect of proton pump inhibition on the gastric volume: assessed by magnetic resonance imaging. Aliment. Pharmacol. Ther. 29, 863–870. https://doi.org/10.1111/j.1365-2036.2009.03947.x.

Bou-Chacra, N., Melo, K.J.C., Morales, I.A.C., Stippler, E.S., Kesisoglou, F., Yazdanian, M., Löbenberg, R., 2017. Evolution of choice of solubility and dissolution media after two decades of biopharmaceutical classification system. AAPS J. 19, 989–1001. https://doi.org/10.1208/s12248-017-0085-5.

Brouwers, J., Brewster, M.E., Augustijns, P., 2009. Supersaturating drug delivery systems: the answer to solubility-limited oral bioavailability? J. Pharm. Sci. 98, 2549–2572. https://doi.org/10.1002/jps.21650.

Brouwers, J., Geboers, S., Mols, R., Tack, J., Augustijns, P., 2017. Gastrointestinal behavior of itraconazole in humans – Part 1: supersaturation from a solid dispersion and a cyclodextrin-based solution. Int. J. Pharm. 525, 211–217. https://doi.org/10.1016/j.ijpharm.2017.04.029.

Chen, B., Zhu, L., Zhang, F., Qiu, Y., Qiu, Yihong, Chen, Y., Zhang, G.G.Z., Yu, L., 2017. Developing solid oral dosage forms (second edition). In: Mantri, R.V (Ed.), Chapter 31 - Process Development and Scale-Up: Twin-Screw Extrusion. Academic Press, Boston, pp. 821–868. https://doi.org/10.1016/B978-0-12-802447-8.00031-5.

Chuasuwan, B., Binjesoh, V., Polli, J.E., Zhang, H., Amidon, G.L., Junginger, H.E., Midha, K.K., Shah, V.P., Stavchansky, S., Dressman, J.B., Barends, D.M., 2009. Biowaiver monographs for immediate release solid oral dosage forms: diclofenac sodium and diclofenac potassium. J. Pharm. Sci. 98, 1206–1219. https://doi.org/10.1002/jps.21525.

Davies, N.M., Anderson, K.E., 1997. Clinical pharmacokinetics of diclofenac therapeutic insights and pitfalls. Clin. Pharmacokinet. 33, 184–213.

de Waal, T., Rubbens, J., Grimm, M., Vandecaveye, V., Tack, J., Weitschies, W., Brouwers, J., Augustijns, P., 2020. Exploring the effect of esomeprazole on gastric and duodenal fluid volumes and absorption of ritonavir. Pharmaceutics 12, 670. https://doi.org/10.3390/pharmaceutics12070670.

Denissen, J.F., Grabowski, B.A., Johnson, M.K., Buko, A.M., Kempf, D.J., Thomas, S.B., Surber, B.W., 1997. Metabolism and disposition of the HIV-1 Protease Inhibitor Ritonavir (ABT-538) in Rats, Dogs, and Humans. Drug Metab. Dispos. 25, 489.

Guhmann, M., Thommes, M., Gerber, F., Pöllinger, N., Klein, S., Breitkreutz, J., Weitschies, W., 2013. Design of biorelevant test setups for the prediction of diclofenac in vivo features after oral administration. Pharm. Res. 30, 1483–1501. https://doi.org/10.1007/s11095-013-0974-y.

Gursoy, O., Memiş, D., Sut, N., 2008. Effect of proton pump inhibitors on gastric juice volume, gastric pH and gastric intramucosal pH in critically ill patients: a randomized, double-blind, placebo-controlled study. Clin. Drug Investig. 28, 777–782. https://doi.org/10.2165/0044011-200828120-00005.

Hens, B., Brouwers, J., Corsetti, M., Augustijns, P., 2016. Supersaturation and precipitation of posaconazole upon entry in the upper small intestine in humans. J. Pharm. Sci. 105, 2677–2684. https://doi.org/10.1002/jps.24690.

Hens, B., Talattof, A., Paixão, P., Bermejo, M., Tsume, Y., Löbenberg, R., Amidon, G.L., 2018. Measuring the impact of gastrointestinal variables on the systemic outcome of two suspensions of posaconazole by a PBPK Model. AAPS J. 20, 57. https://doi.org/10.1208/s12248-018-0217-6.

Hinz, B., Chevts, J., Renner, B., Wuttke, H., Rau, T., Schmidt, A., Szelenyi, I., Brune, K., Werner, U., 2005. Bioavailability of diclofenac potassium at low doses. Br. J. Clin. Pharmacol. 59, 80–84. https://doi.org/10.1111/j.1365-2125.2005.02226.x.

Hsu, A., Granneman, G.R., Bertz, R.J., Laboratories, A., Park, A., 1998. Ritonavir: clinical Pharmacokinetics and Interactions with Other Anti-HIV Agents. Clin. Pharmacokinet. 35, 275–291.

Jamei, M., Abrahamsson, B., Brown, J., Bevernage, J., Bolger, M.B., Heimbach, T., Karlsson, E., Kotzagiorgis, E., Lindahl, A., McAllister, M., Mullin, J.M., Pepin, X., Tistaert, C., Turner, D.B., Kesisoglou, F., 2020. Current status and future opportunities for incorporation of dissolution data in PBPK modeling for pharmaceutical development and regulatory applications: orBiTo consortium commentary. Eur. J. Pharm. Biopharm. 155, 55–68. https://doi.org/10.1016/j.ejpb.2020.08.005.

Jamei, M., Turner, D., Yang, J., Neuhoff, S., Polak, S., Rostami-Hodjegan, A., Tucker, G., 2009. Population-based mechanistic prediction of oral drug absorption. AAPS J. 11, 225–237. https://doi.org/10.1208/s12248-009-9099-y.

Jankovic, S., O' Dwyer, P.J., Box, K.J., Imanidis, G., Reppas, C., Kuentz, M., 2019. Biphasic drug release testing coupled with diffusing wave spectroscopy for mechanistic understanding of solid dispersion performance. Eur. J. Pharm. Sci. 137 https://doi.org/10.1016/j.ejps.2019.105001.

Klein, S., Shah, V.P., 2008. A standardized mini paddle apparatus as an alternative to the standard paddle. AAPS PharmSciTech 9, 1179–1184. https://doi.org/10.1208/s12249-008-9161-6.

Koudriakova, T., Iatsimirskaia, E., Utkin, I., Gangl, E., Vouros, P., Storozhuk, E., Orza, D., Marinina, J., Gerber, N., Ohio, T., 1998. Indinavir and ritonavir by human intestinal microsomes and expressed cytochrome p450 3A4/3A5 : mechanism-based inactivation of cytochrome p4503A by ritonavir. DRUG Metab. Dispos. 26, 552–561.

Kourentas, A., Vertzoni, M., Barmpatsalou, V., Augustijns, P., Beato, S., Butler, J., Holm, R., Ouwerkerk, N., Rosenberg, J., Tajiri, T., Tannergren, C., Symillides, M., Reppas, C., 2018. The BioGIT System: a valuable in vitro tool to assess the impact of dose and formulation on early exposure to low solubility drugs after oral administration. AAPS J. 20, 71. https://doi.org/10.1208/s12248-018-0231-8.

Kourentas, A., Vertzoni, M., Stavrinoudakis, N., Symillidis, A., Brouwers, J., Augustijns, P., Reppas, C., Symillides, M., 2016. An in vitro biorelevant gastrointestinal transfer (BioGIT) system for forecasting concentrations in the fasted upper small intestine: design, implementation, and evaluation. Eur. J. Pharm. Sci. 82, 106–114. https://doi.org/10.1016/j.ejps.2015.11.012.

Litou, C., Patel, N., Turner, D.B., Kostewicz, E., Kuentz, M., Box, K.J., Dressman, J., 2019. Combining biorelevant in vitro and in silico tools to simulate and better understand the in vivo performance of a nano-sized formulation of aprepitant in the fasted and fed states. Eur. J. Pharm. Sci. 138, 105031 https://doi.org/10.1016/j.ejps.2019.105031.

Litou, C., Turner, D.B., Holmstock, N., Ceulemans, J., Box, K.J., Kostewicz, E., Kuentz, M., Holm, R., Dressman, J., 2020. Combining biorelevant in vitro and in silico tools to investigate the in vivo performance of the amorphous solid dispersion formulation of etravirine in the fed state. Eur. J. Pharm. Sci. 105297 https://doi.org/10.1016/j.ejps.2020.105297.

Litou, C., Vertzoni, M., Goumas, C., Vasdekis, V., Xu, W., Kesisoglou, F., Reppas, C., 2016. Characteristics of the human upper gastrointestinal contents in the fasted state under hypo- and a-chlorhydric gastric conditions under conditions of typical drug – drug interaction studies. Pharm. Res. 33, 1399–1412. https://doi.org/10.1007/s11095-016-1882-8.

Litou, C., Vertzoni, M., Xu, W., Kesisoglou, F., Reppas, C., 2017. The impact of reduced gastric acid secretion on dissolution of salts of weak bases in the fasted upper gastrointestinal lumen : data in biorelevant media and in human aspirates. Eur. J. Pharm. Biopharm. 115, 94–101. https://doi.org/10.1016/j.ejpb.2017.02.009.

Markopoulos, C., Andreas, C.J., Vertzoni, M., Dressman, J., Reppas, C., 2015. In-vitro simulation of luminal conditions for evaluation of performance of oral drug products: choosing the appropriate test media. Eur. J. Pharm. Biopharm. 93, 173–182. https://doi.org/10.1016/j.ejpb.2015.03.009.

Marzo, A., Dal Bo, L., Verga, F., Ceppi Monti, N., Abbondati, G., Tettamanti, R.A., Crivelli, F., Uhr, M.R., Ismaili, S., 2000. Pharmacokinetics of diclofenac after oral administration of its potassium salt in sachet and tablet formulations. Arzneimittelforschung 50, 43–47. https://doi.org/10.1055/s-0031-1300162.

McAllister, M., 2010. Dynamic dissolution: a step closer to predictive dissolution testing? Mol. Pharm. 7, 1374–1387. https://doi.org/10.1021/mp1001203.

Miller, D.A., Keen, J.M., Brough, C., Ellenberger, D.J., Cisneros, M., Williams III, R.O., McGinity, J.W., 2016. Bioavailability enhancement of a BCS IV compound via an amorphous combination product containing ritonavir. J. Pharm. Pharmacol. 68, 678–691. https://doi.org/10.1111/jphp.12478.

Morcos, P.N., Moreira, S.A., Navarro, M.T., Bech, N., Quatkemeyer, A., Smith, P.F., Brennan, B.J., 2014. Effect of meal and antisecretory agents on the pharmacokinetics of danoprevir/ritonavir in healthy volunteers. J. Pharm. Pharmacol. 66, 23–31. https://doi.org/10.1111/jphp.12151.

Ng, J., Klein, C.E., Chui, Y.L., Awni, W.M., Morris, J.B., Podsadecki, T.J., Cui, Y., Bernstein, B., Kim, D., 2008. The effect of food on ritonavir bioavailability following administration of ritonavir 100 mg film-coated tablet in healthy adult subjects. J. Int. AIDS Soc. 11, P247. https://doi.org/10.1186/1758-2652-11-S1-P247.

O'Dwyer, P.J., Imanidis, G., Box, K.J., Reppas, C., 2020. On the usefulness of two small-scale in vitro setups in the evaluation of luminal precipitation of lipophilic weak bases in early formulation development. Pharmaceutics 12. https://doi.org/10.3390/pharmaceutics12030272.

O'Dwyer, P.J., Litou, C., Box, K.J., Dressman, J.B., Kostewicz, E.S., Kuentz, M., Reppas, C., 2019. In vitro methods to assess drug precipitation in the fasted small intestine – a PEARRL review. J. Pharm. Pharmacol. 71 https://doi.org/10.1111/jphp.12951.

Pathak, S.M., Ruff, A., Kostewicz, E.S., Patel, N., Turner, D.B., Jamei, M., 2017. Model-based analysis of biopharmaceutic experiments to improve mechanistic oral absorption modeling: an integrated in vitro in vivo extrapolation perspective using Ketoconazole as a model drug. Mol. Pharm. 14, 4305–4320. https://doi.org/10.1021/acs.molpharmaceut.7b00406.

Pathak, S.M., Schaefer, K.J., Jamei, M., Turner, D.B., 2019. Biopharmaceutic IVIVE mechanistic modeling of single- and two-phase in vitro experiments to obtain drug-specific parameters for incorporation into PBPK Models. J. Pharm. Sci. 108, 1604–1618. https://doi.org/10.1016/j.xphs.2018.11.034.

Poulin, P., Theil, F., 2009. Development of a novel method for predicting human volume of distribution at steady-state of basic drugs and comparative assessment with existing methods. J. Pharm. Sci. 98, 4941–4961. https://doi.org/10.1002/jps.

Psachoulias, D., Vertzoni, M., Goumas, K., Kalioras, V., Beato, S., Butler, J., Reppas, C., 2011. Precipitation in and supersaturation of contents of the upper small intestine after administration of two weak bases to fasted adults. Pharm. Res. 28, 3145–3158. https://doi.org/10.1007/s11095-011-0506-6.

Rowland, M., Tozer, T.N., 1995. Clinical pharmacokinetics: concepts and applications, 3rd ed.

Rubbens, J., Mols, R., Brouwers, J., Augustijns, P., 2018. Exploring gastric drug absorption in fasted and fed state rats. Int. J. Pharm. 548, 636–641. https://doi.org/10.1016/J.IJPHARM.2018.07.017.

Segregur, D., Barker, R., Mann, J., Moir, A., Karlsson, E.M., Turner, D.B., Arora, S., Dressman, J., 2021. Evaluating the impact of acid-reducing agents on drug absorption using biorelevant in vitro tools and PBPK modeling - case example dipyridamole. Eur. J. Pharm. Sci. 160, 105750 https://doi.org/10.1016/J.EJPS.2021.105750.

Segregur, D., Flanagan, T., Mann, J., Moir, A., Karlsson, E.M., Hoch, M., Carlile, D., Sayah-Jeanne, S., Dressman, J., 2019. Impact of acid-reducing agents on gastrointestinal physiology and design of biorelevant dissolution tests to reflect these changes. J. Pharm. Sci. 108, 3461–3477. https://doi.org/10.1016/J.XPHS.2019.06.021.

Tang, W.E.I., Stearns, R.A., Kwei, G.Y., Iliff, S.A., Miller, R.R., Egan, M.A., Yu, N.X., Dean, D.C., Kumar, S., Shou, M., Lin, J.H., Baillie, T.A., Metabolism, D., 1999. Interaction of diclofenac and quinidine in monkeys : stimulation of diclofenac metabolism. J. Pharmacol. Exp. Ther. 291, 1068–1074.

Van Den Abeele, J., Brouwers, J., Mattheus, R., Tack, J., Augustijns, P., 2016. Gastrointestinal behavior of weakly acidic BCS class II drugs in man - case study of diclofenac potassium. J. Pharm. Sci. 105, 687–696. https://doi.org/10.1002/jps.24647.

Van Den Abeele, J., Kostantini, C., Barker, R., Kourentas, A., Mann, J.C., Vertzoni, M., Beato, S., Reppas, C., Tack, J., Augustijns, P., 2020. The effect of reduced gastric acid secretion on the gastrointestinal disposition of a ritonavir amorphous solid dispersion in fasted healthy volunteers: an in vivo - in vitro investigation. Eur. J. Pharm. Sci. 151 https://doi.org/10.1016/j.ejps.2020.105377.

Van Den Abeele, J., Schilderink, R., Schneider, F., Mols, R., Minekus, M., Weitschies, W., Brouwers, J., Tack, J., Augustijns, P., 2017. Gastrointestinal and systemic disposition of diclofenac under fasted and fed state conditions supporting the evaluation of in vitro predictive tools. Mol. Pharm. 14, 4220–4232. https://doi.org/10.1021/acs.molpharmaceut.7b00253.

Vidon, N., Pfeiffer, A., Godbillon, J., Rongier, M., Gauron, S., Hirtz, J., Bernier, J., Dubois, J., 1989. Evaluation of the gastric absorption and emptying of drugs under various pH conditions using a simple intubation method: application to diclofenac. Br. J. Clin. Pharmacol. 28, 121–124. https://doi.org/10.1111/J.1365-2125.1989.TB03515.X.

Willis, J.V., Kendall, M.J., Flinn, R.M., Thornhill, D.P., Welling, P.G., 1979. The pharmacokinetics of diclofenac sodium following intravenous and oral administration. Eur. J. Clin. Pharmacol. 16, 405–410.

Wisdom Pharmaceutical Technology Co Limited, 2020. Voltfast sachets 50 mg powder for oral solution summary of product characteristics.

Xu, H., Vela, S., Shi, Y., Marroum, P., Gao, P., 2017. In Vitro characterization of ritonavir drug products and correlation to human in vivo performance. Mol. Pharm. 14, 3801–3814. https://doi.org/10.1021/acs.molpharmaceut.7b00552.